HHS Public Access

Author manuscript

Stroke. Author manuscript; available in PMC 2016 June 01.

Published in final edited form as:

Stroke. 2015 June ; 46(6): 1681–1689. doi:10.1161/STROKEAHA.115.009099.

Mitochondrial Crisis in Cerebrovascular Endothelial Cells Opens the Blood-Brain Barrier

Danielle N. Doll, BSc[1], **Heng Hu, MD**[2,3], **Jiahong Sun, BSc**[3], **Sara E. Lewis, MS**[2,3], **James W. Simpkins, PhD**[2,3], and **Dr. Xuefang Ren, Med.**[2,3,*]

[1]Department of Neurobiology and Anatomy, West Virginia University, Morgantown, West Virginia, 26506 USA

[2]Experimental Stroke Core, Center for Basic and Translational Stroke Research, West Virginia University, Morgantown, West Virginia, 26506 USA

[3]Department of Physiology and Pharmacology, West Virginia University, Morgantown, West Virginia, 26506 USA

Abstract

Background and Purpose—The blood-brain barrier (BBB) is a selectively permeable cerebrovascular endothelial barrier that maintains homeostasis between the periphery and central nervous system (CNS). BBB disruption is a consequence of ischemic stroke and BBB permeability can be altered by infection/inflammation, but the complex cellular and molecular changes that result in this BBB alteration need to be elucidated to determine mechanisms.

Methods—Infection mimic (LPS) challenge on infarct volume, BBB permeability, infiltrated neutrophils and functional outcomes following murine transient middle cerebral artery occlusion (tMCAO) *in vivo*; mitochondrial evaluation of cerebrovascular endothelial cells (CVECs) challenged by LPS *in vitro*; pharmacological inhibition of mitochondria on BBB permeability *in vitro* and *in vivo*; the effects of mitochondrial inhibitor on BBB permeability, infarct volume and functional outcomes following tMCAO.

Results—We report here that LPS worsens ischemic stroke outcome and increases BBB permeability following tMCAO in mice. Further, we elucidate a novel mechanism that compromised mitochondrial function accounts for increased BBB permeability as evidenced by: LPS-induced reductions in oxidative phosphorylation and subunit expression of respiratory chain complexes in CVECs, a compromised BBB permeability induced by pharmacological inhibition of mitochondrial function in CVECs *in vitro* and in an *in vivo* animal model, and worsened stroke outcomes in tMCAO mice following inhibition of mitochondrial function.

Conclusions—We concluded that mitochondria are key players in BBB permeability. These novel findings suggest a potential new therapeutic strategy for ischemic stroke by endothelial cell mitochondrial regulation.

[*]**Correspondence to:** Xuefang Ren, Dr. Med. Address: Biomedical Research Center Rm.109, One Medical Center Dr. PO Box 9229, Morgantown, WV 26506 USA Fax: 1-304-293-3850 Tel: 1-304-581-1892 xuren@hsc.wvu.edu.

Disclosures

None.

Keywords

Mitochondria; Blood-Brain Barrier; Stroke

Introduction

The blood-brain barrier (BBB) is a highly specialized vascular interface that maintains homeostasis in brain by separating the blood compartment from the central nervous system (CNS). Disruption of cerebrovascular endothelial cells not only allows entry of unwanted solutes into brain, but also disrupts the normal CNS entry route of critical nutrients.[1, 2] Disruption and/or dysfunction of the BBB has been observed in cerebrovascular diseases and neurodegenerative disorders such as stroke, Alzheimer's disease (AD), Parkinson disease (PD), Huntington's disease and epilepsy.[3]

Stroke is the second leading cause of death and the leading cause of disability worldwide.[4] It is estimated that 30-40% of all strokes occur during or recently after an acute infection.[5] Acute infections initiate rapid inflammation, and post-stroke infections worsen outcomes in patients[6] and in animal models.[7] However, the mechanisms of this exacerbation by infection on acute stroke outcome are not completely understood.

Ischemia and reperfusion events result in complex cellular and molecular changes that further need to be elucidated. Thus far, studies have provided evidence that the release of oxidants, proteolytic enzymes and inflammatory cytokines alter BBB permeability. The BBB excludes the majority of bacteria; however, similar to ischemia and reperfusion, inflammation induced by bacteria alters BBB permeability. Lipopolysaccharide (LPS) has been shown to disrupt the BBB *in vivo* and *in vitro*, however, how LPS exerts its effects on the BBB is under debate.[8] Previous studies found that an LPS challenge results in a larger infarct volume[7], impairs survival and disrupts BBB[9] in experimental stroke models, through mechanisms that are proposed to involve cytokines.

In the present study, we provide the first evidence that the exacerbation of stroke outcome by a bacterial infection mimic is due to a novel mechanism of compromised cerebrovascular endothelial mitochondrial function. Potential deleterious mitochondrial responses to ischemia have been observed, such as rapid changes in ATP, the release of cytochrome *c*, and the induction of the mitochondrial permeability transition.[10, 11] It is apparent mitochondria play a pivotal role during ischemia; however, the contributions of mitochondrial dysfunction in non-neuronal cells and the interactions between these cells and neurons are poorly understood. Additionally, the involvement of mitochondria in ischemic damage has not been fully elucidated. We show that pharmacological disruption of endothelial mitochondrial function recapitulates all aspects of the LPS exacerbation of stroke, including disruption of the BBB, and worsening of stroke outcome. This discovery could provide a previously unknown mitochondrial-dependent mechanism for acute stroke damage that may offer new therapeutic directions for the treatment of acute stroke.

Methods

Mice

All procedures were conducted according to the criteria approved by the Institutional Animal Care and Use Committees (IACUC) at the West Virginia University (WVU). C57/BL6J male mice (3-4 months old, 25-30g, Jackson Laboratories) were used for all studies.

Anesthesia

All surgical anesthesia was induced with 4-5% isoflurane until the animal showed no response to a toe pinch, and was maintained with 1-2% isoflurane via face-mask in O2-enriched air.

Randomization and blinding of the animal experiments

To assign pre-treatments of mice, we numbered the animals and applied a simple randomization by using excel-generated random numbers. To avoid biases, we also assured that different pre-treatments were performed on the same day. The experimenters were blinded to the pre-treatments and data analysis.

Drug administration

In a subgroup of mice, LPS (Escherichia coli 055:B5, 100 μg/kg, Sigma) dissolved in saline (B. Braun Medical Inc. Irvine, California) was injected intraperitoneally 30 min prior to tMCAO or sham surgery. In another subgroup of mice, rotenone (1 mg/kg, Sigma) was administered intraperitoneally 30 min prior to tMCAO. In the EA model, rotenone (2 mg/ml, 2 μl) was topically applied to the epidural membrane. An equal volume of saline was administered to control mice.

Ischemic model and sham surgery

We performed focal cerebral ischemia for 30 min or 60 min by occlusion of the right middle cerebral artery with a 6.0 monofilament suture (Doccol, Sharon, Massachusetts). We used laser Doppler flowmetry (Moor instruments, United Kingdom) to detect regional cerebral blood flow and confirm a successful occlusion (>70% decrease in flow). Rectal body temperature was maintained at 37 ± 0.5 °C during surgery. Mice were euthanized at several time points as indicated in the text.

Neurological deficits

Neurologic deficit was determined daily before and after tMCAO according to a 0-5 point scale neurological score system as published.[12]

Epidural application (EA) model

We induced anesthesia with 4% isofluorane and maintained with 1% isofluorane. We placed the animal in a prone position under a stereo dissecting microscope and made an incision down the midline of the head and retracted the skin then removed the fascia from the skull. Using a sharp blade, we thinned an area of the skull approximately 0.3-0.5 mm in diameter,

divided the thinned area into several segments, performed a craniotomy by gently removing the thinned skull segments, applied drug or vehicle, and closed the incision.

Exclusion criteria for animal experiments

The exclusion criteria for tMCAO were: 1) regional cerebral blood flow decreases <70% during occlusion as detected by laser Doppler flowmetry; 2) surgery time lasts more than 30 minutes; 3) no neurological deficits 3 hour after MCAO (neurological score 0); 4) no infarction in the MCA territory on TTC staining; 5) subarachnoid hemorrhage on postmortem examination; and 6) substantial ambient temperature change in the animal facility. Animals which died prior to the planned time of assessments were postmortem examined for subarachnoid hemorrhage, and the mortality was recorded.

The exclusion criteria for EA model were: 1) damaged epidural membrane, 2) bleeding from the epidural membrane; 3) the leakage of cerebrospinal fluid from the epidural membrane; 4) body temperature >39.5°C within post-surgery 3 hours; and 5) death.

In this study, 7 mice were excluded: 2 mice (one vehicle and one LPS pre-treatment) because of subarachnoid hemorrhage, 4 mice (2 vehicle and 2 LPS pre-treatment) because the animal facility air conditioner broke down on the day that the experiments were performed, 1 mouse (pre-treated with rotenone) because LDF did not reach 70% reduction during the occlusion. The animal numbers included in the results are 18 vehicle and 23 LPS for 30 min tMCAO mice (4 LPS pretreated mice died), 12 vehicle and 12 rotenone for 60 min tMCAO mice, 5 vehicle and 5 rotenone for EA mice. No animals were excluded in EA model.

Analysis of brain infarct volume

Mice were euthanized with isofluorane. We removed the brains and cut 2 mm coronal sections with a mouse brain matrix. We stained the sections with 2% 2,3,5-triphenyltetrazolium chloride (TTC, Sigma, Saint Louis, Missouri) in phosphate buffer solution (PBS) at 37°C for 30 minutes then fixed the tissue in 10% formalin phosphate buffer for digital photograph. We analyzed the digitized image of each brain section using a computerized image analysis software (ImageJ, NIH) in a double blinded manner. To minimize the effect of brain edema, the volume was expressed as a percentage of contralateral cortex, striatum, and total hemisphere.

Blood-brain barrier (BBB) permeability assay in vivo

The permeability of the BBB was determined by measuring the penetration of Evans blue (Sigma) in the brain tissue. Evans blue (2% in saline, 4 ml/kg body weight) was administered intravenously via the tail vein one hour prior to measurement. The anesthetized animals were perfused transcardially with saline before sampling. Each sample was weighed and homogenized with 400 μl PBS, then precipitated by 50% trichloroacetic acid overnight. The samples were centrifuged for 30 minutes at 10,000 rpm to pellet brain tissue. Absorption of the supernatant was measured at a wavelength of 610 nm with a plate reader (BioTek, Winooski, Vermont). The extravasation of Evans blue was quantified as μg/g brain tissue with an Evans blue standardized curve.

Isolation of immune cells in the blood, spleen and brain

Blood was collected via cardiac puncture then brain and spleen were sampled after transcardial perfusion with saline. Peripheral blood mononuclear cells and splenocytes were prepared by using red cell lysis buffer (eBioscience, San Diego, California). For brain immune cells, the forebrain was dissected from the cerebellum and suspended in RPMI-1640 medium (Corning, Pittsburgh, Pennsylvania). The suspension was digested with type IV collagenase (1 mg/ml, MP Biomedicals, Solon, Ohio) and DNase I (50 μg/ml, Roche Diagnostics, Indianapolis, Indiana) at 37°C for 45 min, then immune cells were isolated by 37–70% Percoll (GE Healthcare, Piscataway, New Jersey) density gradient centrifugation and collected from the interface. Single cell suspension was washed with staining buffer (PBS containing 0.1% NaN3 and 2% FCS) and stained with CD45 (30-F11, eBioscience), CD11b (M1/70, eBioscience), and Gr1 (IA8, BD Bioscience). Propidium iodide (PI, 2 μg/ml, Sigma) was used to exclude dead cells. Appropriate isotype control antibodies were applied to set quadrants for calculating the percentage of positive cells. Data were acquired on FACS Calibur (BD) and analyzed with FlowJo software (TreeStar, Ashland, Oregon).

Cell culture

The bEnd.3 cell line (CRL-2299 from ATCC, Manassas, Virginia) was originally derived from mouse brain cortex endothelial cells and confirmed by the observed major phenotypic features of the blood-brain barrier.[13] Passages 25-30 were used in the study. The bEnd.3 cells were routinely grown in high glucose Dulbecco's modified Eagle's medium (DMEM, ATCC) supplemented with 10% FCS and 1% penicillin/streptomycin (Hyclone, South Logan, Utah) at 37 °C in 5% CO2 humid atmosphere. Mouse primary brain microvascular endothelial cells (B129-7023 from CellBiologics, Chicago, Illinois) were routinely grown in complete Endothelial Cell Medium (Cell Biologics, M1168) at 37 °C in 5% CO2 humid atmosphere.

Blood-brain barrier permeability assay in vitro

Permeability assays were performed in triplicate as follows: 1.5×10^5 endothelial cells were grown on transwell inserts (pore size: 0.4 mm, diameter: 6.5mm, Millipore, Darmstadt, Germany) for two days, 250 μg/ml FITC labelled dextran FD-70 (70 kDa, Sigma) was added to the apical side of the filters and the medium in the basolateral compartment was sampled every 15 min for 2 hours. The FD-70 permeability through the cultured endothelial monolayer was determined directly by analysis of the apparent permeability coefficient (Papp).[14] The concentration of FD-70 was determined with an FD-70 standard curve on plate reader (Ex. 490 nm, Em. 515 nm). Papp (cm/s) was calculated.

Oxygen Consumption

Oxygen consumption rate (OCR) was measured at 37 °C using an XF96e extracellular analyzer (Seahorse Bioscience, North Billerica, Massachusetts) according to the manufacturer's instructions. Briefly, the bEnd.3 cells or primary endothelial cells were seeded into Seahorse Bioscience XF96e cell culture plates (16,000 cells/well) in 80 μl medium and allowed to adhere and grow overnight in the 37 °C humidified incubator with

5% CO2. Then the cells were supplied with 80 μl medium with or without LPS (concentration varies as indicated in the text) and cultured for additional 24 hours. For the measurements of extracellular flux, the medium was changed 1 h prior to the start of the extracellular flux assay to un-buffered (pH 7.4) DMEM containing 2 mM GlutaMax, 1 mM sodium pyruvate, and 25 mM glucose and incubated at 37 °C without CO2. Oligomycin, carbonyl cyanide 4-(trifluoromethoxy) phenylhydrazone (FCCP), rotenone and antimycin A (all from Sigma) and 10× dilutions were prepared for the assays. A sensor cartridge was loaded with 20 μl of oligomycin (10 μM) into Port A, 20 μl of FCCP (30 μM) into Port B, 20 μl of Rotenone (20 μM) and antimycin A (20 μM) into Port C. The Sensor cartridge was calibrated and equilibrated and then the protocol was implemented on an XF96e Analyzer. This protocol allowed determination of the basal level of oxygen consumption, the amount of oxygen consumption linked to ATP production, the maximal respiration capacity, and the non-mitochondrial oxygen consumption.

Detect respiratory chain complex I-IV by flow cytometry

We cultured cells in 6 well plates and treated cells with LPS (1 μg/ml) for 48 hours, then we washed cells and performed intracellular staining with an intracellular staining set (cat. 72-5775, eBioscience). We stained cells with anti-rabbit-NADH-dehydrogenase-ubiquinone-1-alpha-subcomplex-assembly-factor-1 (NDUFAF1, sc-292085, 1:100, Santa Crutz), anti-mouse-NADH-dehydrogenase-ubiquinone-1-subunit-C2 (NDUFC2, sc-393771, 1:100, Santa Crutz), anti-mouse-NADH-dehydrogenase-ubiquinone-ironsulfur-protein-2 (NDUFS2, sc-390596, 1:100, Santa Crutz), anti-rabbit-Succinate-dehydrogenase (SDH, cat. 11998, 1:100, Cell signaling, Beverly, Massachusetts), anti-rabbit-Cytochrome c (Cyc, cat. 4280, 1:100, Cell signaling), anti-mouse-Cytochrome c oxidase (COX IV, cat. 4850, 1:100, Cell signaling) antibodies for 30 min and labeled the cells with a proper second antibody, PE-anti-rabbit (Cat.8885, 1:100, Cell signaling) or PE-anti-mouse (Cat.8887, 1:500, Cell signaling). We acquired data on BD Calibur flow cytometry and analyzed mean fluorescence intensity by Flowjo software.

Immunohistochemistry staining

To perform the immunohistochemistry co-staining of mitochondria and MyD88, the bEnd.3 cells were cultured on cover slips, stained with mitotracker (Life technologies, Grand Island, New York) for 30 minutes, washed with PBS then fixed with 2% paraformaldehyde (PFA, Polysciences, Inc.) for 10 minutes at 37 °C. The cells were blocked with 5% goat serum staining buffer and stained with anti-rabbit-MyD88 (1:200, Abcam, Cambridge, Massachusetts) overnight, then washed with PBS and stained with goat-anti-rabbit-FITC (Life technologies) for 2 hours. The cells were further washed with PBS and mounted on glass slides using prolong gold anti-fade reagent (Life technologies). The slides were photographed with confocal LSM 510 microscope Zeiss (Zeiss, Oberkochen, Germany) using software ZEN 2012.

Statistical Analysis

Statistical analysis was performed with Prism 5 software (Graphpad software, La Jolla, California). Differences between groups were analyzed by the unpaired Student's t-test, one way ANOVA or two way ANOVA as indicated in the figure legends.

Results

LPS increases cerebral infarction and BBB permeability in stroke

To test the effects of a bacterial infection mimic on stroke outcome, we performed intraperitoneal (i.p.) injections of LPS (100 μg/kg) or saline 30 minutes prior to a 30-minute transient middle cerebral artery occlusion (tMCAO) in mice (**Fig. 1A**). LPS challenge significantly increased infarct volume in the cortex (P = 0.04), striatum (P = 0.009) and total hemisphere (P = 0.04) after 30 minute tMCAO followed by 48 hour reperfusion (**Fig. 1B, C**).

However, the time course of post-stroke BBB leakage, whether biphasic or progressive, remains subject to debate.[15, 16] Using Evans Blue as a tracer, our recent work demonstrated biphasic peaks of BBB openings at 6 hours and 72 hours but not at 24 hours or 48 hours reperfusion following one hour tMCAO.[17] The 6-hours-peak of BBB opening may suggest the early inflammatory infiltration and brain edema in acute stroke. Thus, to determine if the acute infection challenge regulates cerebrovascular response to stroke, we compared the effects of LPS vs. saline on Evans blue extravasation at 6 hours reperfusion following tMCAO (**Fig. 2A**). Six hours after tMCAO (30 min occlusion), mice were perfused and isolated brains were divided into ipsilateral and contralateral hemispheres, and each hemisphere was analyzed separately for Evans blue extravasation. LPS significantly increased Evans blue extravasation in the ipsilateral hemisphere after tMCAO compared to control mice (**Fig. 2B**), indicating that LPS enhances cerebrovascular permeability after stroke.

LPS increases neutrophil infiltration into the injured brain in stroke

Stroke and acute infections elicit inflammatory responses in the injured brain that are mediated by multiple factors. Neutrophils are among the first peripheral cells to infiltrate ischemic brain tissue within 30 minutes to a few hours after focal cerebral ischemia, and neutrophil infiltration is believed to contribute to acute phase damage in stroke.[18] To assess brain leukocyte invasion, we measured neutrophils in brain and peripheral tissues by flow cytometry. Neutrophil accumulation in the ipsilateral and contralateral brain hemispheres was significantly greater in the LPS group compared to saline control ($n = 5$, $P < 0.05$) at 6 hours tMCAO post reperfusion (**Fig. 2C**). Concurrently, fewer neutrophils and greater lymphocytes were detected in the peripheral blood and spleen but monocytes did not differ between vehicle and LPS treated mice (**supplemental Figure I A, C**). The neutrophil to lymphocyte ratio (NLR) was significantly decreased in the blood ($n = 5$, $P = 0.02$), and spleen ($n = 5$, $P = 0.004$) of LPS-treated mice (**supplemental Figure I B, D**). tMCAO mice with LPS exhibited worsened neurological score at all end point experiments ($P = 0.0005$, **Fig. 2D**), and mortality was higher in LPS versus saline tMCAO mice (4/23 vs. 0/18, respectively). Although neutrophil accumulation in the CNS is complex, these data are consistent with the LPS increased BBB permeability after tMCAO.

LPS impairs mitochondrial oxidative phosphorylation in CVECs

To determine if the LPS effects in stroke are due to direct effects on cerebrovascular endothelial cells, we employed a cultured cerebrovascular endothelial cell (cCVEC) model.

Immunohistochemical staining showed that CD31 (an endothelial cell marker) and TLR4 (a LPS receptor) colocalize in the brain vasculature (**supplemental Figure II A**), closely resembling the expression of CD31 and TLR4 on cCVECs (**supplemental Figure II B**). This indicates that cCVECs have critical components for an *in vitro* model to investigate LPS effects on cerebrovascular endothelial cells.

The brain has a high energy demand and elevated mitochondrial content resulting in it being vulnerable to reductions in oxidative phosphorylation. Given the expression of TLR4 on the brain vascular endothelial cells, we determined if LPS would directly affect oxidative phosphorylation and mitochondrial capacity in CVECs. Using Mitotracker Red for visualization of mitochondria, we detected MyD88, an adaptor protein involved in TLR4 signaling,[19] broadly distributed but also colocalized with mitochondria in cCVECs (**Fig. 3A**), suggesting that LPS-induced signaling pathways are linked to mitochondria. To directly evaluate the mitochondrial function in cCVECs affected by LPS, a bioenergetic assay was used to examine cellular energetic oxygen consumption rates (OCR). Basal OCR did not significantly differ in cCVECs challenged by LPS for 24 hours, but maximal respiration and spare capacity were significantly reduced in cCVECs cultured with 0.1-100 μg/ml LPS (**Fig. 3B & supplemental Figure III A**). Similarly, in primary cerebrovascular endothelial cells (pCVECs), an LPS challenge for 24 hours resulted in a decrease in maximal respiration and spare capacity at 100 μg/ml (**Fig. 3C** & **supplemental Figure III B)**. However, reduced oxidative phosphorylation was not associated with cell death or cell viability in cCVECs or pCVECs, as evidenced by PI staining (**supplemental Figure IV A&B**), calcein AM staining **(supplemental Figure IV C&D**) for 24 hours in the exception of high dose of LPS (100 μg/ml). In view of the LPS effects on mitochondrial respiration, respiratory chain complex I proteins (NADH dehydrogenase ubiquinone subunits: NDUFAF1, NDUFS2 and NDUFA2), complex II protein (Succinate dehydrogenase, SDH), complex III protein (cytochrome c, Cyc), and complex IV protein (Cytochrome c oxidase, COX IV) were examined after a 1 μg/ml LPS challenge for 48 hours, and flow cytometry confirmed that LPS decreases the expression of complex I (NDUFS2 and NDUFA2), complex III (Cyc) and complex IV (COX IV) (**Fig. 3D**) proteins. Together these results strongly suggest that oxidative phosphorylation of CVECs is compromised with LPS exposure, and this effect does not induce endothelial cell death. As such, we asked if mitochondrial activity affects endothelial cell function.

Impaired mitochondria disrupt CVEC tight junction and increase BBB permeability

It is known that LPS impairs the BBB permeability both *in vitro* and *in vivo* at doses which are thought to be caused by inflammatory mediators such as cytokines,[8] but little is known about the role of mitochondria in BBB integrity. Using a pharmacological strategy to manipulate mitochondrial respiration, we first demonstrated that inhibition of respiratory chain complex I with rotenone (**Fig. 4A**), uncoupling of electron flow from ATP production with FCCP (**Fig. 4B**), or inhibition of complex V with oligomycin (**Fig. 4C**) rapidly increased FITC-dextran 70 permeability in a cCVEC monolayer transwell system *in vitro*. Immunocytochemical analysis revealed that the normally well-defined, linear cell-cell junctions were disrupted when oxidative phosphorylation was inhibited by mitochondrial inhibitors (**Fig. 4D**). Both increased permeability and cell-cell junction disruption due to

inhibition of oxidative phosphorylation occurred in the absence of cell death as evidenced by PI staining (**supplemental Figure V A**) and calcein AM staining (**supplemental Figure V B**). These data suggest for the first time that mitochondria play a key role in maintaining BBB integrity *in vitro*.

To determine if inhibition of mitochondria affects the BBB permeability *in vivo*, we developed an epidural application model for CNS drug administration in mice (**Fig. 5A-D**). This model permits local drug delivery without traumatic brain injury (**Fig. 5C**), thus allowing assessment of BBB permeability. Rotenone (2μl, 2mg/ml dissolved in saline) was applied to the epidural surface, and BBB permeability was evaluated by Evans blue quantification after 6 hours. Mice treated with rotenone showed significantly higher Evans blue extravasation than vehicle controls (**Fig. 5D**). These data support the hypothesis that mitochondria are critical for the regulation of cerebrovascular permeability *in vivo*.

Inhibition of mitochondrial function worsens stroke severity in mice

If inhibition of mitochondrial function increases BBB permeability, the same perturbation would be expected to affect infarct size and stroke severity. When we treated mice with rotenone prior to tMCAO (**Fig. 6A**), increased BBB permeability (**Fig. 6B**) and infarct volumes (**Fig. 6C**), and worsened neurological deficits (**Fig. 6D**) were observed. Thus, the LPS-induced exacerbation of stroke outcome most likely is due to the deleterious effect of mitochondrial inhibition.

Discussion

Acute systemic infection is a risk factor and/or trigger for human stroke[5, 6] and is associated with worsened clinical outcome [20]. Although much is known about the factors that worsen stroke severity in clinical subjects and experimental stroke models, less is understood about their mechanisms. Our data are the first to demonstrate that a bacterial infection mimic acts with ischemic challenge to markedly exacerbate stroke damage via a mitochondrial-dependent mechanism. This new finding could also provide an explanation for the association of infections with severity of brain damage and BBB dysfunction from stroke: the induction of hypometabolism in cerebrovascular endothelial cell mitochondria.

Mitochondrial dysfunction is increasingly recognized as an accomplice in vascular diseases and ischemic stroke. More recently, it has been shown that components of the TLR4 signaling pathways, MyD88 and TRAF6, are linked with mitochondria and affect oxidative phosphorylation.[21] The expression of MyD88 in mitochondria of endothelial cells (**Fig. 3A**) supports that mitochondrial function can be affected by LPS (**Fig. 3B&C**). It is notable that no significant effect of LPS is seen on cCVEC basal oxygen consumption and ATP-linked oxygen consumption upon treatment with oligomycin (**Fig. 3B & supplemental Figure III**), indicating that LPS does not significantly change basal oxygen demand in mitochondria after 24 hours of treatment with LPS. However, the loss of maximal respiration and spare capacity (**Fig. 3B & supplemental Figure III**) demonstrates that mitochondrial capacity is reduced by LPS and thus the effects exacerbate the mitochondrial impairment by ischemia. Cellular respiration, mitochondrial biogenesis and function, require coordinated expression of proteins encoded by nuclear and mitochondrial genes including mitochondrial complex I-

IV. The reduced expression of respiratory chain complex I, III and IV proteins in cCVECs by LPS provides further evidence that LPS compromises the endothelial mitochondria function (**Fig. 3D**).

The 30 minute tMCAO model mimics a mild ischemic event that results in a small infarct (**Fig. 1C**) and does not cause visible BBB disruption at 6 hours reperfusion (**Fig. 2B**). The bacterial infection mimic challenge prior to tMCAO increased BBB permeability (**Fig. 2B**) and exacerbated infarct volume (**Fig. 1C**). There are inconsistent data for LPS- or cytokine-induced BBB dysfunction[8] that may be due to complex mechanisms. McColl *et al.*[7] demonstrated an interleukin-1-dependent mechanism of stroke exacerbation using the same LPS-tMCAO model. Others have demonstrated that LPS alters transporters or enzymes involved in BBB maintenance.[22] Our observation that pharmacological inhibition of mitochondria disrupts BBB integrity and increases BBB permeability *in vitro* **(Fig. 4**) and *in vivo* **(Fig. 5**) strengthens the argument that BBB permeability is increased by LPS after stroke (**Fig. 2**) through a direct mitochondrial mechanism resulting in a larger infarct volume and worsening neurological deficit.

Increased BBB permeability, is positively correlated with massive vasogenic and cytotoxic edema post-stroke[23, 24] and elevated neutrophils in the ischemic area that contribute to infarct expansion[25] and poor clinical outcome.[26] Our observation of neutropenia and low NLR may be a consequence of BBB damage that causes rapid migration of neutrophils into damaged tissue. Brain infiltration of neutrophils could also account for secondary lesion growth and increased infarct size in the ischemic brain as seen with LPS treatment (**Fig. 1C**). These data may provide translational evidence that neutropenia and low NLR may predict severe stroke.

We observed that LPS-induced inhibition of mitochondria exacerbates infarct volume and opens BBB in tMCAO mice (**Fig. 1&2**), but that mitochondria inhibition in cCVECs and pCVECs does not affect cell viability in 24 hours (**supplemental Figure IV**). This suggests that the functional impairment of endothelial mitochondria by LPS may be reversible and an effective intervention could be designed to prevent/restore BBB during strokes. However, our data also indicated that a high dose of LPS (100 μg/ml) induced cell death and reduced cell viability in cCVECs (**supplemental Figure IV**), and extension of LPS exposure for 48 hours induced cell death in both cCVECs and pCVECs (**supplemental Figure IV A-D**). Therefore, the effective mitochondrial directed intervention may be limited by the severity or the length of the infectious exposure to rescue BBB damage.

Leukocytosis, and cytokine and chemokine storm are features of the acute-phase reaction in systemic infections and in acute stroke. It is becoming increasingly apparent that inflammation can disturb cell energy metabolism. Our recent study found that neuronal mitochondrial function was rapidly and profoundly decreased by TNF-α resulting in neuronal cell death.[27] Another study demonstrated that TNF-α elevated oxygen consumption rate in endothelial cells.[28] The present study did not address the complex LPS-induced effects on mitochondria, however, our novel findings refreshed the traditional idea of infection-inflammation responses and provided a new explanation for the LPS effects on BBB dysfunction: a direct mitochondrial-dependent mechanism.

The application of rotenone on the epidural surface argues that its effect on BBB opening is by compromised mitochondria in vascular endothelial cells (**Fig. 5**). Rotenone exposure is associated with clinical features of parkinsonism in humans[29], and broadly used to induce PD like-symptoms in animal models[30] as well. This suggests that the mitochondrial-dependent BBB opening may not only involve in the progress of stroke but also other neurodegenerative disorders such as PD and AD.

In summary, the present study describes a previously unknown mechanism of infection-induced direct mitochondrial dysfunction in cerebrovascular endothelial cells, which compromises BBB permeability and exacerbates acute stroke outcomes. Moreover, our observations argue that maintenance of mitochondrial function is critical to the integrity of the BBB. The data also suggest a translational significance: maintenance of brain endothelial cell mitochondrial function can improve the acute outcome of stroke and perhaps other neurodegenerative diseases.

Supplementary Material

Refer to Web version on PubMed Central for supplementary material.

Acknowledgments

The authors thank Dr. Linda Van Eldik (University of Kentucky) and Dr. Paul Lockman (WVU) for their critical pre-review of the manuscript. We acknowledge Dr. Jeffrey Wimsatt and Dr. Matthew Kessler for their advice on IACUC protocol.

Sources of Funding

This work was supported by NIH (P20 GM109098, P01 AG027956, U54 GM104942, and T32 GM081741). Imaging experiments were performed at the West Virginia University (WVU) Microscope Imaging Facility supported by the Mary Babb Randolph Cancer Center (MBRCC) and NIH (P20 RR016440, P30 RR032138/GM103488 and P20 RR016477). Flow cytometry was performed at the WVU Flow Cytometry Core Facility supported by MBRCC and NIH (P30 RR032138/GM103488 and GM103434).

References

1. Rubin LL, Staddon JM. The cell biology of the blood-brain barrier. Annual review of neuroscience. 1999; 22:11–28.
2. Gonzalez-Mariscal L, Betanzos A, Avila-Flores A. Maguk proteins: Structure and role in the tight junction. Seminars in cell & developmental biology. 2000; 11:315–324. [PubMed: 10966866]
3. Tajes M, Ramos-Fernandez E, Weng-Jiang X, Bosch-Morato M, Guivernau B, Eraso-Pichot A, et al. The blood-brain barrier: Structure, function and therapeutic approaches to cross it. Molecular membrane biology. 2014; 31:152–167. [PubMed: 25046533]
4. Feigin VL, Forouzanfar MH, Krishnamurthi R, Mensah GA, Connor M, Bennett DA, et al. Global and regional burden of stroke during 1990-2010: Findings from the global burden of disease study 2010. Lancet. 2014; 383:245–254. [PubMed: 24449944]
5. Grau AJ, Buggle F, Heindl S, Steichen-Wiehn C, Banerjee T, Maiwald M, et al. Recent infection as a risk factor for cerebrovascular ischemia. Stroke; a journal of cerebral circulation. 1995; 26:373–379.
6. Grau AJ, Buggle F, Steichen-Wiehn C, Heindl S, Banerjee T, Seitz R, et al. Clinical and biochemical analysis in infection-associated stroke. Stroke; a journal of cerebral circulation. 1995; 26:1520–1526.
7. McColl BW, Rothwell NJ, Allan SM. Systemic inflammatory stimulus potentiates the acute phase and cxc chemokine responses to experimental stroke and exacerbates brain damage via

interleukin-1- and neutrophil-dependent mechanisms. The Journal of neuroscience : the official journal of the Society for Neuroscience. 2007; 27:4403–4412. [PubMed: 17442825]

8. Banks WA, Erickson MA. The blood-brain barrier and immune function and dysfunction. Neurobiology of disease. 2010; 37:26–32. [PubMed: 19664708]
9. Denes A, Ferenczi S, Kovacs KJ. Systemic inflammatory challenges compromise survival after experimental stroke via augmenting brain inflammation, blood- brain barrier damage and brain oedema independently of infarct size. Journal of neuroinflammation. 2011; 8:164. [PubMed: 22114895]
10. Sims NR, Muyderman H. Mitochondria, oxidative metabolism and cell death in stroke. Biochimica et biophysica acta. 2010; 1802:80–91. [PubMed: 19751827]
11. Sims NR, Anderson MF. Mitochondrial contributions to tissue damage in stroke. Neurochemistry international. 2002; 40:511–526. [PubMed: 11850108]
12. Harhausen D, Khojasteh U, Stahel PF, Morgan BP, Nietfeld W, Dirnagl U, et al. Membrane attack complex inhibitor cd59a protects against focal cerebral ischemia in mice. Journal of neuroinflammation. 2010; 7:15. [PubMed: 20202211]
13. Brown RC, Morris AP, O'Neil RG. Tight junction protein expression and barrier properties of immortalized mouse brain microvessel endothelial cells. Brain research. 2007; 1130:17–30. [PubMed: 17169347]
14. Artursson P. Epithelial transport of drugs in cell culture. I: A model for studying the passive diffusion of drugs over intestinal absorptive (caco-2) cells. Journal of pharmaceutical sciences. 1990; 79:476–482. [PubMed: 1975619]
15. Sandoval KE, Witt KA. Blood-brain barrier tight junction permeability and ischemic stroke. Neurobiology of disease. 2008; 32:200–219. [PubMed: 18790057]
16. Nag S, Kapadia A, Stewart DJ. Review: Molecular pathogenesis of blood-brain barrier breakdown in acute brain injury. Neuropathology and applied neurobiology. 2011; 37:3–23. [PubMed: 20946242]
17. Hu H, Jun S, Sarkar SN, Doll DN, Ren X, Simpkins JW. Dynamic blood-brain barrier openings concur with increasing of mir-let7a in murine experimental stroke. Society for Neuroscience. 2014; 701.05
18. Gee JM, Kalil A, Shea C, Becker KJ. Lymphocytes: Potential mediators of postischemic injury and neuroprotection. Stroke; a journal of cerebral circulation. 2007; 38:783–788.
19. Gay NJ, Symmons MF, Gangloff M, Bryant CE. Assembly and localization of toll-like receptor signalling complexes. Nature reviews. Immunology. 2014; 14:546–558.
20. Palasik W, Fiszer U, Lechowicz W, Czartoryska B, Krzesiewicz M, Lugowska A. Assessment of relations between clinical outcome of ischemic stroke and activity of inflammatory processes in the acute phase based on examination of selected parameters. European neurology. 2005; 53:188–193. [PubMed: 15956787]
21. Kim Y, Zhou P, Qian L, Chuang JZ, Lee J, Li C, et al. Myd88-5 links mitochondria, microtubules, and jnk3 in neurons and regulates neuronal survival. The Journal of experimental medicine. 2007; 204:2063–2074. [PubMed: 17724133]
22. Banks WA, Dohgu S, Lynch JL, Fleegal-DeMotta MA, Erickson MA, Nakaoke R, et al. Nitric oxide isoenzymes regulate lipopolysaccharide-enhanced insulin transport across the blood-brain barrier. Endocrinology. 2008; 149:1514–1523. [PubMed: 18187549]
23. Yang Y, Rosenberg GA. Blood-brain barrier breakdown in acute and chronic cerebrovascular disease. Stroke; a journal of cerebral circulation. 2011; 42:3323–3328.
24. Taheri S, Candelario-Jalil E, Estrada EY, Rosenberg GA. Spatiotemporal correlations between blood-brain barrier permeability and apparent diffusion coefficient in a rat model of ischemic stroke. PloS one. 2009; 4:e6597. [PubMed: 19668371]
25. Bektas H, Wu TC, Kasam M, Harun N, Sitton CW, Grotta JC, et al. Increased blood-brain barrier permeability on perfusion ct might predict malignant middle cerebral artery infarction. Stroke; a journal of cerebral circulation. 2010; 41:2539–2544.
26. Warach S, Latour LL. Evidence of reperfusion injury, exacerbated by thrombolytic therapy, in human focal brain ischemia using a novel imaging marker of early blood-brain barrier disruption. Stroke; a journal of cerebral circulation. 2004; 35:2659–2661.

27. Doll DN, Rellick SL, Barr TL, Ren X, Simpkins JW. Rapid mitochondrial dysfunction mediates tnf-alpha-induced neurotoxicity. Journal of neurochemistry. 2015; 132:443–451. [PubMed: 25492727]

28. Drabarek B, Dymkowska D, Szczepanowska J, Zablocki K. Tnfalpha affects energy metabolism and stimulates biogenesis of mitochondria in ea.Hy926 endothelial cells. The international journal of biochemistry & cell biology. 2012; 44:1390–1397. [PubMed: 22687752]

29. Tanner CM, Kamel F, Ross GW, Hoppin JA, Goldman SM, Korell M, et al. Rotenone, paraquat, and parkinson's disease. Environmental health perspectives. 2011; 119:866–872. [PubMed: 21269927]

30. Chesselet MF, Richter F. Modelling of parkinson's disease in mice. The Lancet. Neurology. 2011; 10:1108–1118. [PubMed: 22094131]

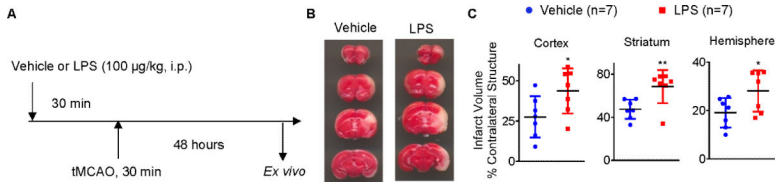

Fig. 1. LPS exacerbates stroke infarct volume in mice

(**A**) Scheme depicting the experimental design. LPS (100 μg/kg, i.p.) or vehicle (saline, i.p.) was administered 30 min prior to right transient middle cerebral artery occlusion (tMCAO; 30 min) and 48 hour reperfusion was performed. (**B**) Infarct volumes were measured at 48 hours after ischemia induction. Representative TTC-stained coronal sections used to analyze infarction of mice treated with vehicle vs. LPS. (**C**) Mice treated with LPS had significantly larger infarct volume than vehicle group in cortex, striatum and total hemisphere. Mean ± S.D.; n = 7 per group; Student's t test. *, $P < 0.05$; **, $P < 0.01$.

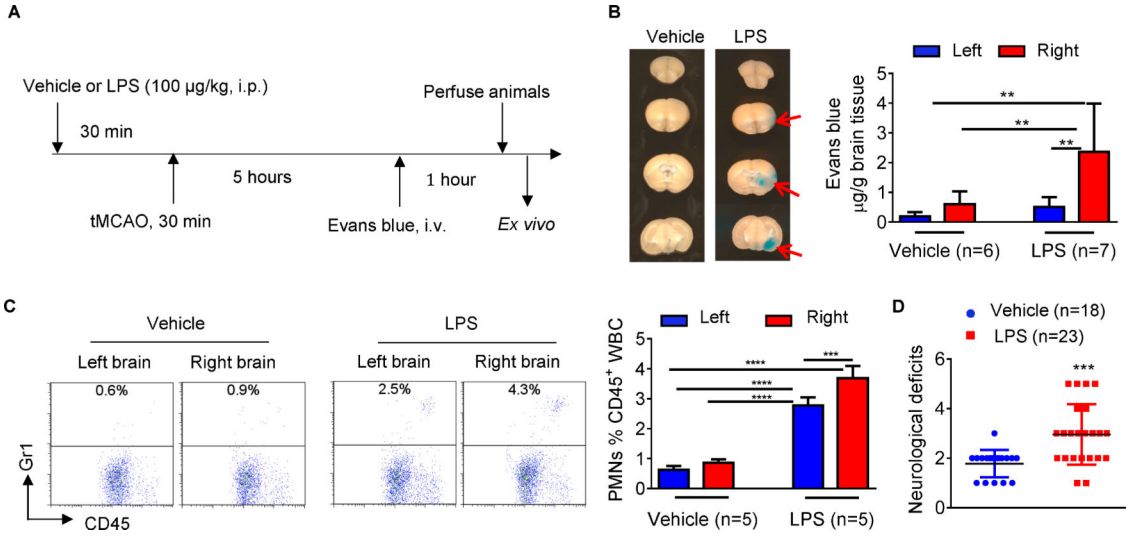

Fig. 2. LPS increases early BBB leakage and infiltration of neutrophils into the brain of stroke mice

(**A**) Scheme of experimental design and workflow. LPS (100 µg/kg, i.p.) or vehicle (saline, i.p.) was administered 30 min prior to right tMCAO (30 min occlusion) and 6 hour reperfusion was performed. (**B**) Evans blue accumulation was visible in the brain of LPS pre-treated stroke mice (Red arrows) and quantification of Evans Blue extravasation (µg/g brain tissue) in contralateral (left) and ipsilateral (right) hemispheres. Vehicle, n = 6; LPS, n = 7. (**C**) Representative FACS data for individual hemispheres from mice treated with vehicle vs. LPS after 30 min tMCAO plus 6 hours reperfusion, and statistical analysis of infiltrated PMNs in the contralateral (left) and ipsilateral (right) hemispheres measured by FACS. N = 5 per group. (**D**) Neurological score at combined two end points (6 hours and 48 hours) after tMCAO. Vehicle, n = 18, LPS, n = 23. Data are expressed as mean ± S.D.; One-way ANOVA followed by post-hoc Tukey's test was used for multiple group comparison and Student's t test was used for two group statistical analysis. (**, $P < 0.01$; ***, $P < 0.001$; ****, $P < 0.0001$.)

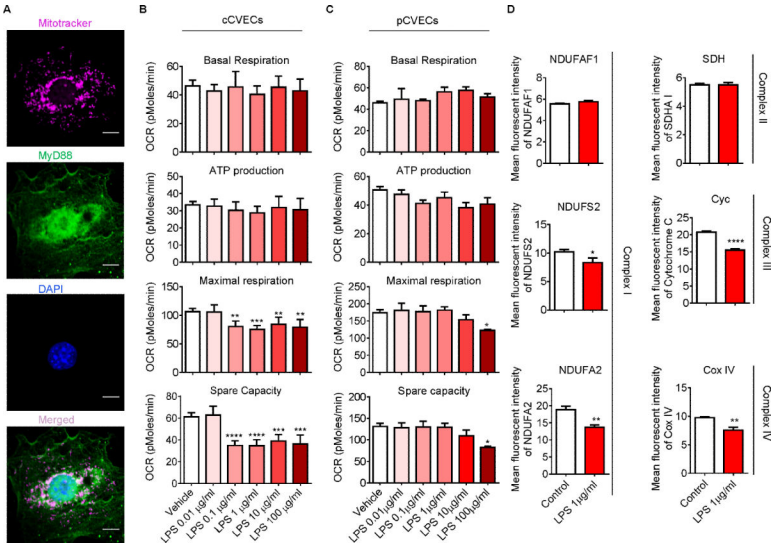

Fig. 3. LPS reduces mitochondrial function in cultured and primary cerebrovascular endothelial cells

(**A**) Immunofluorescence staining of mitochondrial (MitoTracker, purple) co-stained with MyD88 (green), suggests that the MyD88 expresses on mitochondria of cultured cerebral vascular endothelial cells (cCVECs). Nuclei were stained with DAPI (blue). Results are representative from four independent experiments. Images were taken under 63× objective. Scale bars = 10 μm. (**B**) Bioenergetics functional assay in cCVECs exposed to various concentration of LPS compared to vehicle control for 24 hours. Basal respiration, ATP production, maximal respiration, and spare capacity were calculated from the assay presented in **supplementary Figure III A**. Results are representative from four independent experiments. N = 4 per group; **, $P < 0.01$; ***, $P < 0.001$; ****, $P < 0.0001$ vs. vehicle group. One way ANOVA followed by post-hoc Tukey's test was used for data analysis. (**C**) Bioenergetics functional assay in pCVECs exposed to various concentration of LPS compared to vehicle control for 24 hours. Basal respiration, ATP production, maximal respiration, and spare capacity were calculated from the assay presented in **supplementary Figure III B**. Results are representative from four independent experiments. N = 4 per group; *, $P < 0.05$ vs. vehicle group. One way ANOVA followed by post-hoc Tukey's test was used for data analysis. (**D**) Analysis of mitochondrial specific proteins for complex I proteins (NDUFAF1, NDUFS2, NDUFA2), complex II protein (succinate dehydrogenase, SDH), complex III protein (cytochrome c, Cyc), and complex IV protein (cytochrome c oxidase, cox IV) in cCVECs after a 1 μg/ml LPS challenge for 48 hours. Flow cytometry confirmed that LPS decreases the expression of complex I (NDUFS2 and NDUFA2), complex III (cytochrome c) and complex IV (cox IV) proteins. Results are representative from three independent experiments. N = 3 per group; *, $P < 0.05$; **, $P < 0.01$; ****, $P < 0.0001$ vs. vehicle group. Student's t test was used for data analysis.

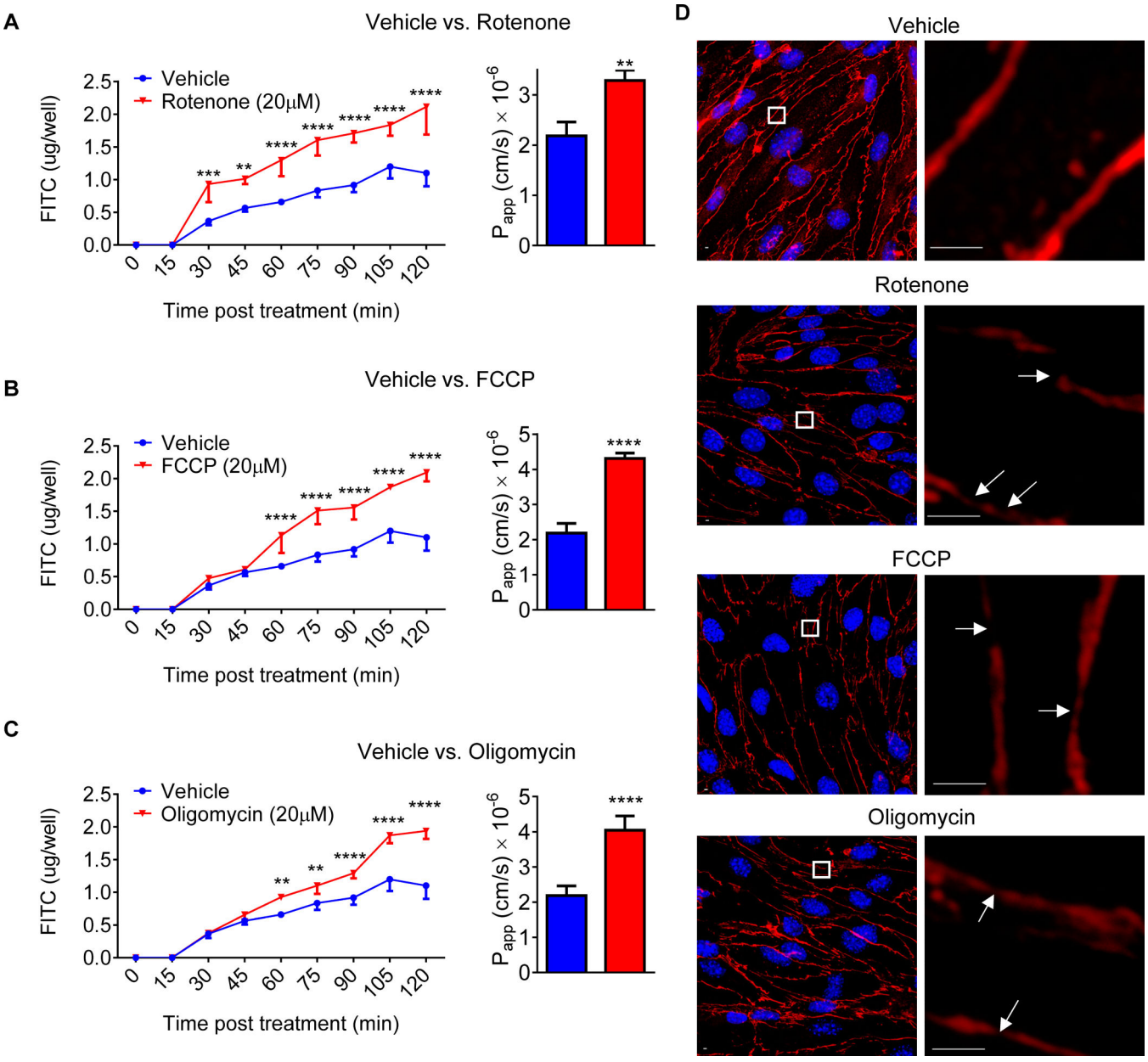

Fig. 4. Pharmacological inhibition of mitochondria increases BBB permeability *in vitro*

FITC-Dextran-70 permeability after addition of 20 μM rotenone (**A**), 20 μM FCCP (**B**) and 20 μM oligomycin (**C**) vs. vehicle to cultured cerebrovascular endothelial cells (cCVECs). Data are presented as both real-time rate of permeability (Two-way ANOVA followed by post-hoc Dunnett's test) and calculated apparent permeability coefficient (*Papp*, Student t-test). N = 3 per group. **, $P < 0.01$; ***, $P < 0.001$; ****, $P < 0.0001$. (**D**) Confocal fluorescence images of cCVEC confluent monolayers after treatment with 20 μM rotenone, 20 μM FCCP and 20 μM oligomycin vs. vehicle for 2 hours. The immunohistochemistry staining of ZO-1 (red) was performed for tight junctions. Nuclei were stained with DAPI (blue). Mitochondrial inhibitors apparently disrupted tight junctions and resulted in gaps between cells (white arrows).

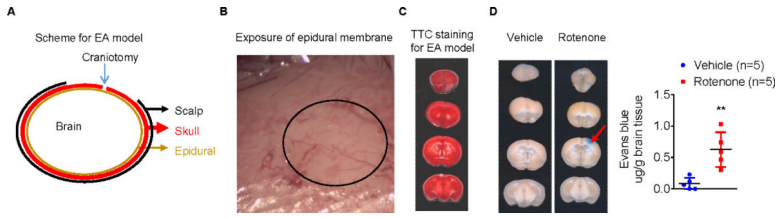

Fig. 5. Pharmacological inhibition of mitochondria increases BBB permeability *in vivo*

(**A**) Graph depicting the epidural application (EA) model. (**B**) Exposure of epidural membrane: vessels were visible under surgical microscope. (**C**) TTC staining in the EA model showing no brain injury. (**D**) Evans blue accumulation was visible in the brain of rotenone applied mice (red arrows) in EA model and quantitative analysis of Evans blue extravasation (μg/g brain tissue) in individual brain. N = 5 per group; One-way ANOVA followed by post-hoc Tukey's test. Data are expressed as mean ± S.D.; **, $P < 0.01$.

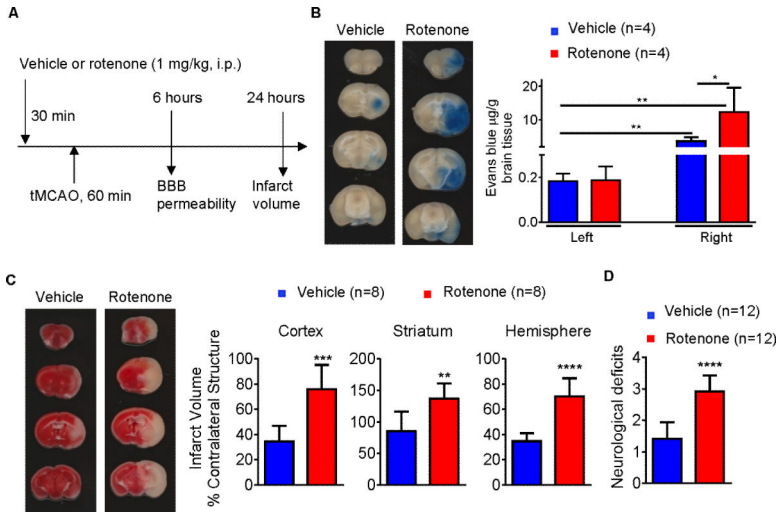

Fig. 6. Impairment of mitochondria function exacerbates stroke outcomes

(A) Scheme of experimental design and workflow. Rotenone (1mg/kg, i.p.) or vehicle (saline, i.p.) was administered 30 min prior to right tMCAO (60 min occlusion), BBB permeability was evaluated at 6 hour reperfusion and infarct volume was measured at 24 hour reperfusion. (**B**) Representative brain coronal sections for Evans blue accumulation and quantitative analysis of Evans Blue extravasation (µg/g brain tissue) in contralateral (left) and ipsilateral (right) hemispheres. Vehicle, n = 4; Rotenone, n = 4. One-way Data are analyzed with ANOVA followed by post-hoc Tukey's test *(*, $P < 0.05$)*. (**C**) Representative TTC-stained coronal sections used to analyze infarct of tMCAO mice and quantitative analysis of infarct volumes. Mice treated with rotenone had significant larger infarct volume than vehicle group, in cortex, striatum, and total hemisphere. Rotenone (1 mg/kg, i.p.) or vehicle (saline, i.p.) was administered 30 min prior to right tMCAO (1 hour occlusion) and 24 hour reperfusion was performed. Vehicle, n = 8; Rotenone, n = 8. Data are analyzed with Student's t tests *(**, $P < 0.01$; ***, $P < 0.001$; ****, $P < 0.0001$.)*. (**D**) Rotenone worsened neurological deficits at 6 and 24 hours after tMCAO. Vehicle, n = 12; Rotenone, n = 12. Data are analyzed with Student's t test *(****, $P < 0.0001$)*.